Redox Biology 39 (2021) 101832

Contents lists available at ScienceDirect

Redox Biology

journal homepage: www.elsevier.com/locate/redox

Research Paper

An inherent dysfunction in soluble guanylyl cyclase is present in the airway of severe asthmatics and is associated with aberrant redox enzyme expression and compromised NO-cGMP signaling

Arnab Ghosh [a,*], Cynthia J. Koziol-White [b], William F. Jester Jr. [b], Serpil C. Erzurum [a], Kewal Asosingh [a], Reynold A. Panettieri Jr. [b], Dennis J. Stuehr [a,**]

[a] Department of Inflammation and Immunity, Lerner Research Institute, The Cleveland Clinic, Cleveland, OH, 44195, USA
[b] Rutgers Institute for Translational Medicine and Science, Rutgers University, New Brunswick, NJ, 08901, USA

ARTICLE INFO

JEL classification:
Inflammation
Cell Signaling

Keywords:
Bronchodilation
Smooth muscle
Cytochrome *b*5 reductase
Catalase
Thioredoxin
Reactive oxygen
Nitric oxide

ABSTRACT

A subset of asthmatics develop a severe form of the disease whose etiology involves airway inflammation along with inherent drivers that remain ill-defined. To address this, we studied human airway smooth muscle cells (HASMC), whose relaxation drives airway bronchodilation and whose dysfunction contributes to airway obstruction and hypersensitivity in severe asthma. Because HASMC relaxation can be driven by the NO-soluble guanylyl cyclase (sGC)-cGMP signaling pathway, we questioned if HASMC from severe asthma donors might possess inherent defects in their sGC or in redox enzymes that support sGC function. We analyzed HASMC primary lines derived from 17 severe asthma and 16 normal donors and corresponding lung tissue samples regarding sGC activation by NO or by pharmacologic agonists, and also determined expression levels of sGC α1 and β1 subunits, supporting redox enzymes, and related proteins. We found a majority of the severe asthma donor HASMC (12/17) and lung samples primarily expressed a dysfunctional sGC that was NO-unresponsive and had low heterodimer content and high Hsp90 association. This sGC phenotype correlated with lower expression levels of the supporting redox enzymes cytochrome *b*5 reductase, catalase, and thioredoxin-1, and higher expression of heme oxygenases 1 and 2. Together, our work reveals that severe asthmatics are predisposed toward defective NO-sGC-cGMP signaling in their airway smooth muscle due to an inherent sGC dysfunction, which in turn is associated with inherent changes in the cell redox enzymes that impact sGC maturation and function.

1. Introduction

Asthma is a growing health problem that is estimated to impact 300 million people worldwide [1,2]. A subset of asthma patients (approximately 5–10%) manifest severe disease often characterized by irreversible airway obstruction, frequent exacerbations and/or a significant oral corticosteroid burden [3,4]. Although airway inflammation is thought to play a role in severe asthma, inherent dysfunction in the airway epithelial and/or smooth muscle cells, which are pivotal in regulating bronchomotor tone, may also contribute to the asthma diathesis [4–8].

Human airway smooth muscle cells (HASMC) play a central role in bronchomotor function and in asthma their dysregulation promotes the airway narrowing, obstruction and hypersensitivity that characterizes the disease [6,9]. The β_2-adrenergic-adenylyl cyclase-cAMP signaling pathway (β_2AR-sAC-cAMP) that is present in the HASMC modulates bronchomotor tone [10] and is the target of current bronchodilator therapy. HASMC also express soluble guanylyl cyclase (sGC), which by signaling through the nitric oxide (NO)-sGC-cyclic GMP (cGMP) pathway also promotes HASMC relaxation and bronchodilation [11,12]. The NO-sGC-cGMP pathway is the primary driver of vascular smooth muscle relaxation [13–15], and its role in HASMC relaxation has long

* Corresponding author. Department of Inflammation and Immunity/NC22, Lerner Research Institute, The Cleveland Clinic, 9500 Euclid Ave., Cleveland, OH, 44195, USA.
** Corresponding author. Department of Inflammation and Immunity/NC22, Lerner Research Institute, The Cleveland Clinic, 9500 Euclid Ave, Cleveland, OH, 44195, USA.
E-mail addresses: ghosha3@ccf.org (A. Ghosh), stuehrd@ccf.org (D.J. Stuehr).

https://doi.org/10.1016/j.redox.2020.101832
Received 29 October 2020; Received in revised form 5 December 2020; Accepted 8 December 2020
Available online 13 December 2020

been suspected [16]. However, it was only recently established that activating this pathway is as efficacious in evoking bronchodilation in human small airways as is activating the β_2AR-sAC-cAMP pathway [12,17].

Both of the signaling pathways in HASMC that drive bronchodilation can become attenuated in asthma. This typically manifests as defective β_2-adrenergic receptor recycling [18] or as development of sGC insensitivity toward NO activation [11]. NO-insensitive sGC is thought to arise *in situ* from the increased oxidative and nitrosative stress that is present in the inflamed airways. For example, in murine models of allergen-induced airway inflammation, the airway sGC developed hallmarks of damage that include dissociation of its active heterodimeric form and an association of its freed sGCβ1 subunit with heat shock protein 90 (hsp90), a cell chaperone [11]. In the human asthmatic airway, such *in situ* oxidative damage to sGC could occur in addition to any underlying genetic or epigenetic factors that might compromise the HASMC signaling pathways independent of the airway inflammation. Indeed, GWAS studies indicate that there are altered gene expression patterns in human asthma that associate with disease severity [4,19]. Despite this, how genetic predisposition or epigenetic changes may impair the bronchodilation signaling pathways in HASMC remains largely unexplored.

Here, we posited that primary HASMC lines derived from severe asthmatic donors (SA-HASMC), but not those from non-asthma donors (N-HASMC), may manifest inherently dysfunctional NO-sGC-cGMP signaling, which could lead to an aberrant HASMC phenotype consistent with asthma. To explore this, we focused on sGC and performed pharmacologic profiling of its activation by NO or by two pharmacores in a number of SA-HASMC and N-HASMC lines and lung tissues derived from severe asthma and non-asthma donors. Also, because gene expression analyses have limitations in studies of airway smooth muscle dysfunction due to many of their functional properties being regulated at the protein level [20], we performed protein expression studies in the HASMC and lung tissues as a means to identify abnormalities linked to severe asthma. In this regard, we determined the protein expression levels of the two sGC subunits, cell chaperone hsp90, phosphodiesterase 5A (PDE5A), cGMP-dependent protein kinase 1(PKG-1), and five redox enzymes that are known to impact sGC maturation and function: cytochrome *b*5 reductase isoform 3 (CYB5R3), catalase, thioredoxin 1 (Trx1), and heme oxygenases 1 and 2 (HO1 and HO2). Our findings reveal that the airway smooth muscle of many severe asthmatics harbors defective NO-sGC-cGMP signaling, due to an inherent sGC dysfunction that correlates with an altered expression of the redox enzymes that govern sGC maturation and NO response.

2. Material and methods

Reagents, cells and tissues: All chemicals were purchased from Sigma (St. Louis, MO) and Fischer chemicals (New Jersey). NO donor, S-Nitroso-N-Acetyl-D,L-Penicillamine (SNAP), phosphodiesterase inhibitor 3-isobutyl-1-methylxanthine (IBMX) and sGC activator BAY 41–2272 were all purchased from Sigma. sGC activator BAY 60–2270 was provided by Bayer Pharma. Smooth muscle specific cell culture media was purchased from Lonza. Fetal bovine serum were purchased from Fischer and Atlanta Biologicals. All HASMC lines from normal and severe asthma donors and lung tissue samples were provided by the laboratory of Dr. Rey Panettieri (Rutgers). We used N-HASMC lines derived from 19 different donors and SA-HASMC lines derived from 20 different donors in the study (a total of 39 distinct HASMC lines). Some of these had corresponding lung tissue samples that we analyzed, but not all, which are listed Table S1. We used 12 additional donor lung tissue samples which did not correspond to the 39 HASMC lines. Thus, the HASMC lines plus tissues used in the study derived from a total of 51 different donors. cGMP ELISA assay kits were obtained from Cell Signaling Technology. Catalase activity assay kit was purchased from Biovision. Molecular mass markers were purchased from Biorad. For animal experiments wild type naïve female BALB/c mice 6–8 week old were purchased from the Jackson Laboratory (Bar Harbor, ME).

Antibodies: Table S2 describes various types of antibodies used and their sources.

Cell culture, growth and preparation of human airway smooth muscle cells supernatants: All normal and asthma patient derived HASMCs were grown in 100 mm tissue culture dishes and harvested following procedures as previously described [21,22]. HASMCs were grown in smooth muscle specific culture media from Lonza and following the manufacturer's protocol. A maximum of three passages were used from each set of HASMCs, after which the cultures were discontinued. To enable maximum efficiency of this method by working within this narrow window of cell culture we made multiple parallel liquid nitrogen stocks (10 or more stocks) for each individual HASMCs from the time point of its first culture. This ensured that repeated experiments could be performed from each individual stock of HASMCs without altering its passage number. Experiments on HASMCs eg. in cell activation by NO or sGC activators (BAY-41/60) were performed on confluent (70–80%) cultures before harvest. At the point of cell harvest, the monolayers were washed twice with 4 ml cold PBS containing 1 mg/ml of glucose, and cells on each plate were collected by scraping in presence of 250 μl of classical lysis buffer (40 mM EPPS buffer pH 7.6, 10% Glycerol, 3 mM DTT, 150 mM NaCl and 1% NP40) or at times cell lysis buffer from cGMP estimation kit (Cell Signaling Technology) was used. The collected cells were lysed by 3 cycles of freeze-thawing (in liquid nitrogen and at 37 °C, respectively). The lysates were centrifuged for 30 min at 4 °C and the supernatants were collected and stored at −80 °C. Total protein contents of the supernatants was determined using the Bio-Rad protein assay kit.

Preparation of lung tissue homogenates: Human and mouse lung tissue homogenates were made by incubating about 600 mg of the lung tissue in 1 ml of cell lysis buffer [11] for 30 min in ice, followed by sonication to homogenize the softened tissue. The homogenates were further lysed by 3 cycles of freeze-thawing (in liquid nitrogen and at 37 °C, respectively). The lysates were centrifuged for 30 min at 4 °C and the supernatants were collected and stored at −80 °C. Total protein contents of the supernatants was determined using the Bio-Rad protein assay kit.

Western blots and immunoprecipitations (IPs): Western blots were peformed using standard protocols as previously mentioned [11,21,22]. For westerns involving multiple samples (16 normals and 17 asthma HASMC supernatants), 80 μg of the supernatants from normals or asthma were run separately on two large SDS-PAGE (8% or 15%), transferred to the same PVDF membrane, probed with a specific antibody and developed at the same time. In all cases β-actin was used as a loading control. Multiple protein detection was achieved by stripping the membranes and re-probing with specific antibodies. For immunoprecipitations (IP), 600 μg of the total cell supernatant was precleared with 20 μl of protein G-sepharose beads (Amersham) for 1 h at 4 °C, beads were pelleted, and the supernatants incubated overnight at 4 °C with 3 μg sGCβ1 antibody. Protein G-sepharose beads (20 μL) were then added and incubated for 1 h at 4 °C. The beads were micro-centrifuged (6000 rpm), washed three times with wash buffer (50 mM HEPES pH 7.6, 100 mM NaCl, 1 mM EDTA and 0.5% NP-40) and then boiled with SDS-buffer and centrifuged. The supernatants were then loaded on SDS-PAGE gels and western blotted with specific antibodies. For IPs depicted in Fig. 2 where multiple samples were involved, similar procedures of gel running, transfer and blot development were followed as mentioned earlier. Band intensities on westerns were quantified using Image J quantification software (NIH).

Determination of relative sGC heterodimer levels in cells: To estimate the relative level of sGC heterodimer, the Western blots were scanned to obtain band intensities of the sGCα1 and sGCβ1 bands that were present in each pulldown sample. The relative heterodimer value was calculated as (intensity sGCα1 band/intensity sGCβ1 band) x 100.

cGMP enzyme-linked immunosorbent assay: The cGMP

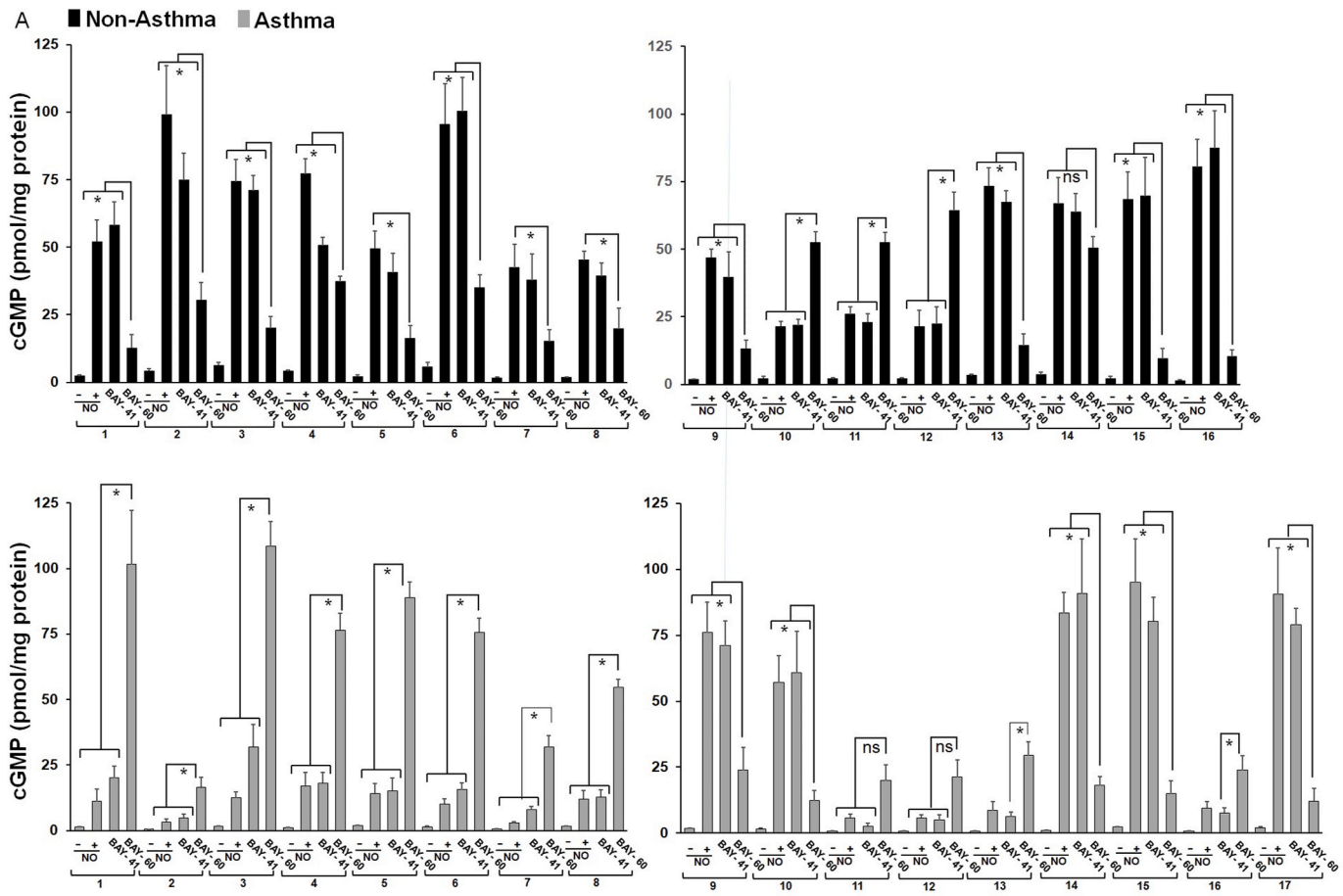

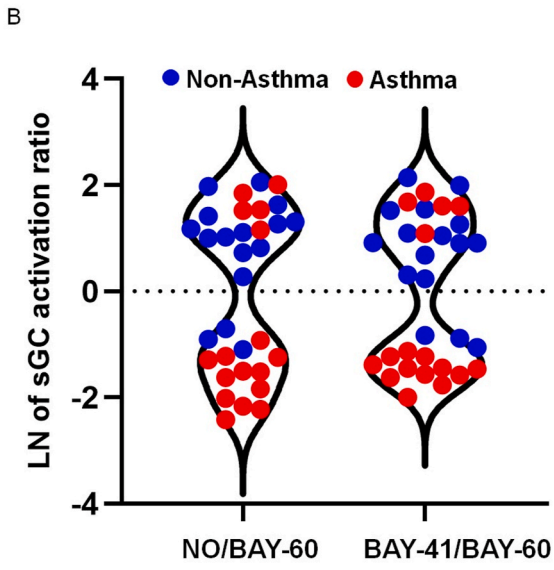

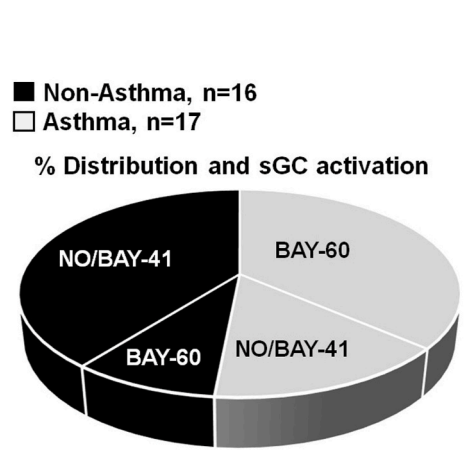

Fig. 1. sGC activation response profiles of HASMC lines isolated from non-asthma or severe asthmatic donors. Sixteen non-asthma HASMC and seventeen asthma HASMC lines were cultured, their sGC underwent no activation or was activated by NO donor, BAY-41, or BAY-60, and their cGMP production measured. (A) cGMP production values. Data are means (n = 3 repeats per condition) ± SD. *p < 0.05, by one-way ANOVA, ns = not significant. (B) Distribution of the indicated sGC activation ratios (in terms of natural log, LN) among all 33 HASMC lines. (C) Distribution of the 33 HASMC lines regarding their being predominantly activated by NO or BAY-41 *versus* BAY-60.

concentration in various cell supernatants made from intact cells that had been given NO from NO donor SNAP (50 μM) or sGC activators (BAY-41/60) in the presence of 250 μM IBMX, was estimated using the cGMP ELISA assay kit (Cell Signaling Technology). sGC activation profile ratios, BAY-41/BAY-60 or vice versa were determined from the mean values of three independent experiments (n = 3). sGC enzymatic activity in human lung tissue supernatants was determined as previously described [21]. Briefly the lung tissue supernatants were passed through

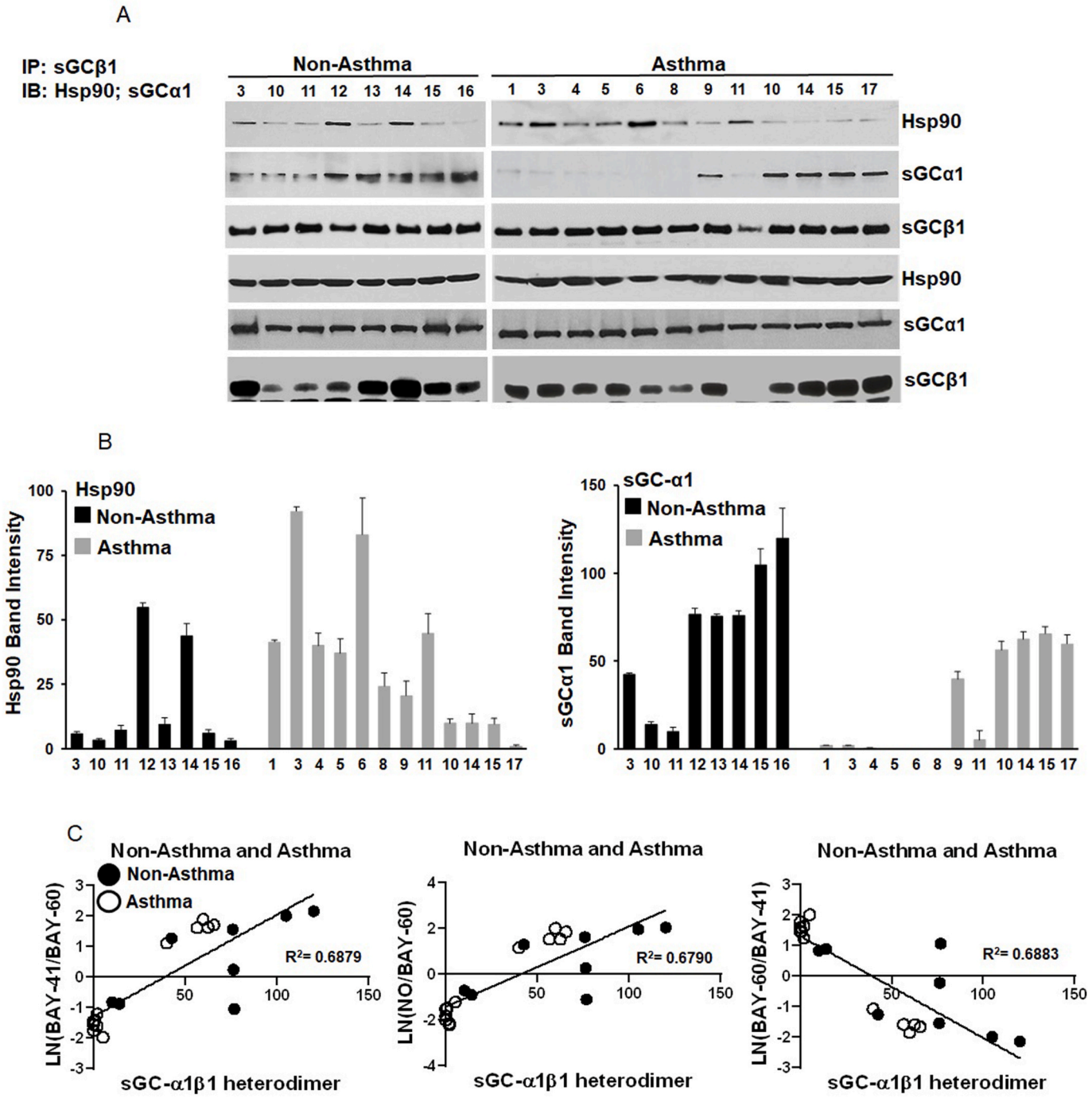

Fig. 2. An aberrant sGC activation response in HASMC lines correlates with their having a diminished sGC-α1β1 heterodimer and an increased hsp90 association. Supernatants were prepared from the designated non-asthma and severe asthma HASMC lines and subject to IP to compare the releative extents of sGC-β1association with sGC-α1 or with hsp90. (A) Representative Western blots from IP pulldowns of sGC-β1. Upper three panels represent the bound proteins in the IP, while the lower three panels depicts protein expression levels in the supernatants. Numbers at the top of the panel depict the corresponding HASMC numbers shown in Fig. 1 (B) Mean densitometries of hsp90 bands (left) and sGCα1 bands (right) associated with sGCβ1 for each HASMC line, after normalizing the hsp90 and sGCα1 band intensities to the intensity of the corresponding sGCβ1 band. Data are mean (n = 3 repeats per condition) ± SD. (C) Relationship between the sGC activation response ratios and the proportion of sGC heterodimer in the HASMC lines. Values are the natural log (LN) of the mean activation ratios (BAY-41/BAY-60, NO/BAY-60, or BAY-60/BAY-41) of the HASMC (calculated from Fig. 1) versus their mean proportion of sGC heterodimer (from data in Panel B). Lines of best fit are shown along with correlation coefficients.

the desalting PD-spin trap G-25 columns (GE healthcare), then activated by adding 250 μM GTP, 10 μM of sGC activators BAY-41 or BAY-60 in the presence of 250 μM IBMX and incubated for 10 min at 37 °C [21]. Reactions were quenched by addition of 10 mM Na_2CO_3 and Zn $(CH_3CO_3)_2$ and the generated cGMP was then determined by ELISA. The cGMP concentrations as determined by ELISA was a measure of sGC activity in the cells.

Catalase Activity assay: Catalase activity assays in the HASMC supernatants was estimated using a Colorimetric assay kit from Biovision. This kit assays catalase activity in biological samples or cell supernantants by allowing the cellular catalase to reduce hydrogen peroxide (H_2O_2) into water (H_2O) and oxygen (O_2). The unconverted H_2O_2 then

reacts with OxiRed™ probe pesent in the kit to produce a product whose absorbance can be measured at 570 nm. Catalase activity was thus inversely proportional to the signal.

Murine asthma model: Allergic airway disease was performed as previously described [11]. For the house dust mite model C57 B l/6 mice were anesthetized by isoflurane inhalation and intranasally sensitized with 100 μg house dust mite extract (HDME) in 50 μl saline. Five days later animals received five daily intranasal challenges of 10 μg HDME in 50 μl saline. Three days later lung airway measurements were made [23] and the animals were sacrificed and lung tissues excised and stored for various biochemical measurements.

3. Results

SA-HASMC predominantly contain NO-insensitive sGC: To test sGC function in the SA-HASMC and N-HASMC lines we compared their sGC activation responses to an NO donor and to the pharmacologic sGC agonists BAY-41 or BAY-60. Cells and tissues typically express a proportion of their sGC in its ferrous heme-containing heterodimeric form, which can only be activated by NO or by pharmacore agonists like BAY-41, and also express a proportion of their sGC in heme-oxidized (ferric) or heme-free forms, which are insensitive to NO or BAY-41 but can be activated by pharmacore agonists like BAY-60 [21,24]. When tissues and cells display greater sGC activation by NO or BAY-41 compared to BAY-60, this indicates that the cells contain sGC predominantly in its NO-responsive, ferrous heme-containing heterodimeric form.

In a preliminary screen that compared 3 SA-HASMC and 3 N-HASMC lines we found that cGMP production by the SA-HASMC lines was more strongly activated by BAY-60 compared to the NO donor or BAY-41, whereas cGMP production by the N-HASMC lines was more strongly activated by NO or BAY-41 (Fig. S1). We also found variable protein expression of sGCβ1 and four other proteins (Hsp90, HO2, Catalase, and Trx1) in our initial screen (Fig. S1). Given these results we expanded our study to include HASMC lines isolated from an additional 17 severe asthma and 16 non-asthma donors, whose cohort information is reported in Fig. S2 and Table S1.

The sGC activation response profiles of the N-HASMC lines (Fig. 1A) show that 13 of 16 generated more cGMP in response to NO donor or BAY-41 as compared to BAY-60. This response profile is typical of other cell types or tissues that express sGC [21,25,26] and implies that the ferrous heme-containing sGC heterodimer predominates in a majority of the cultured primary N-HASMC lines [12,16]. In contrast, we saw the opposite pattern in the SA-HASMC lines, where 12 of the 17 showed greater cGMP generation in response to BAY-60 compared to the NO donor or BAY-41, and some showing a far greater activation by BAY-60 (Fig. 1A).

To better visualize how the 33 HASMC lines distribute regarding their activation by BAY-41 or NO donor *versus* by BAY-60, we used cGMP production data in Fig. 1A to calculate the BAY-41:BAY-60 and the NO:BAY-60 activation ratios, and then plotted the natural log of these ratios in violin distribution plots shown in Fig. 1B. The BAY-41:BAY-60 and the NO:BAY-60 distribution profiles were remarkably similar, consistent with NO and BAY-41 activating the same form of sGC, namely the ferrous heme-containing heterodimer. Both plots show that the HASMC lines distribute between a group whose activation by BAY-41 or by NO predominate over BAY-60, and another group whose activation by BAY-60 predominates. Notably, the former group is heavily populated by the N-HASMC lines, while the latter group is heavily populated by the SA-HASMC lines. These distributions indicate that 81% of the N-HASMC lines were predominantly NO or BAY-41 responsive, compared to only 29% of the SA-HASMC lines (Fig. 1C). The sGC activation profile for each HASMC line is also reported in Table S3. We conclude that most of the SA-HASMC display an aberrant sGC activation response profile that indicates they contain increased levels of NO-unresponsive, and therefore dysfunctional, sGC.

sGC dysfunction is linked to a diminished heterodimer content and to greater sGCβ1-Hsp90 complex formation: To probe the mechanism responsible for the aberrant sGC activation that was seen in some of the HASMC lines, we examined its relationship to an altered heterodimer status. We specifically selected for this analysis 12 SA-HASMC and 8 N-HASMC lines such that five lines in either group were predominantly NO and BAY-41 responsive, and the rest (seven and three lines, respectively) were predominantly BAY-60 responsive. Fig. 2A shows representative immunoprecipitation (IP) and Western blot data that compare the relative levels of sGCα1 or hsp90 that were associated with cell sGCβ1 in pull-down experiments using supernatants made from each HASMC line, while Fig. 2B reports the same information averaged over three replica experiments. All of the N-HASMC lines showed some sGCα1 association with sGCβ1 and varying levels of hsp90 association, indicating that they all contained some sGC heterodimer. Of the three N-HASMC lines that were predominantly BAY 60 responsive [10–12], two showed realtively low levels of sGCα1 association (Fig. 2B), consistent with their containing less sGC in heterodimer form. Among the 12 SA-HASMC lines that we analyzed, the five that we selected based on their having a stronger NO or BAY-41 activation response [9,10,14,15,17] all showed a good level of sGCα1 association and a weaker level of hsp90 association (Fig. 2B), consistent with their containing significant levels of sGC heterodimer. In contrast, the seven SA-HASMC lines that showed predominant BAY 60 activation showed little or no sGCα1 association with sGCβ1 and instead showed a stronger association of hsp90 with sGCβ1. Note that the ability of BAY-60 to activate cGMP production in cells that contain little or no sGC heterodimer is due to BAY-60 activating through binding to the sGCβ1-hsp90 species and driving it to form an active sGC heterodimer in the cells [21].

We next used the sGCα1 and sGCβ1 band intensities in the pulldowns to determine the relative level of sGC heterodimer in each of the 20 HASMC lines that we analyzed. Fig. 2C plots how the BAY-41:BAY-60 activation ratio, the NO:BAY-60 activation ratio, and the BAY-60:BAY-41 activation ratio of the HASMC lines correlate with their relative proportions of sGC heterodimer. The data indicate that a positive correlation generally exists between the sGC heterodimer content and capacity for NO or BAY-41 activation across all of the HASMC lines, while a negative correlation exists between sGC heterodimer content and the capacity for BAY-60 activation. We conclude that the aberrant NO sGC activation response seen in the HASMC lines is in most cases related with their having a lower proportion of sGC in heterodimer form and with a greater proportion of the sGCβ1 subunit being associated with hsp90.

Dysfunctional sGC also exists in lung tissue samples from severe asthmatics: To examine if the aberrant sGC phenotype seen in the cultured SA-HASMC lines also manifests in donor lung tissues, we compared the sGC activation response profiles and heterodimer levels in lung tissue samples (Fig. S3) from 6 normal and 3 severe asthmatic donors. As depicted in Fig. 3A, four of the six normal lung samples had predominant sGC activation by BAY-41 relative to BAY-60, while all three lung tissue samples from severe asthmatics showed predominant sGC activation by BAY-60. We performed IPs on six of these tissue samples to assess the sGCβ1 protein partners (Fig. 3B and C) and found that in the lung samples from non-asthmatic donors there was a relative strong interaction of sGCβ1 with sGCα1 and a weak hsp90 interaction, whereas in the lung samples from severe asthmatics the sGCβ1 association pattern was reversed with hsp90 predominating. Plots of the BAY-41:BAY- 60 or BAY-60:BAY-41 activation ratios obtained with the lung tissues (Fig. 3D) show that an aberrant sGC activation response correlated with a lower proportion of sGC heterodimer. Thus, the HASMC and lung tissues derived from severe asthma donors are similar with regard to their expressing an sGC that has poor heterodimer content, poor activation by NO or BAY-41, and strong activation by BAY-60.

Protein expression profiling indicates variable sGCβ1 expression in severe asthma: We next compared the SA-HASMC and N-HASMC lines regarding their expression levels of sGCβ1, sGCα1, and Hsp90, and two enzymes important for cGMP signaling: PDE5A, which produces GMP to negatively influence NO-sGC-cGMP signaling [27], and PKG-1, which is

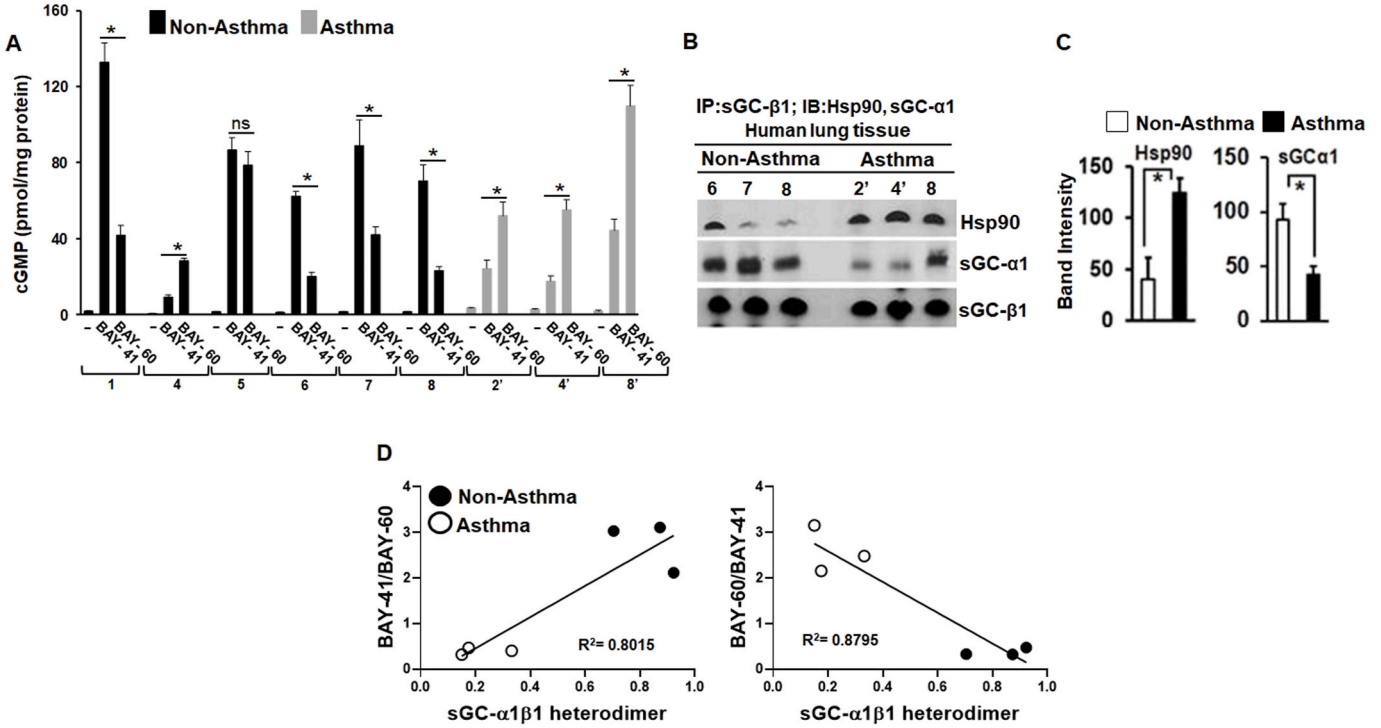

Fig. 3. Lung tissues from severe asthmatics display an aberrant sGC activation response that correlates with a diminished sGC-α1β1 heterodimer and an increased hsp90 association. Supernatants were prepared from lung tissue samples obtained from six non-asthma and three severe asthma donors. (A) cGMP production in response to no stimulus, BAY-41, or BAY-60. (B) IPs and Western analyses were performed with the indicated supernatants to determine the levels of hsp90 and sGC-α1 associated with sGC-β1 (input 20%) retained on the beads. (C) Densitometry of the associated hsp90 and sGC-α1 bands as shown in panel B. Data in Panels A and B are the mean (n = 3 repeats per condition) ± SD. *$p < 0.05$, by one-way ANOVA, ns = not significant. (D) Relationship between the mean BAY-41/BAY-60 or BAY-60/BAY-41 activation ratios and the mean proportions of sGC-α1β1 heterodimer in the six supernatants depicted in Panel B. Lines of best fit are shown along with correlation coefficients. The six control and severe asthma lung tissue samples studied here are also reported on in Fig. S3A.

a down-stream enzyme whose activation by cGMP leads to smooth muscle relaxation [28]. Fig. 4A contains representative Western blots indicating the relative expression levels of these proteins in each HASMC line, while Fig. 4B compares their average expression levels normalized to the corresponding β-actin band intensities from two replica analyses. The protein expression levels are also listed in Table S3.

The level of sGCβ1 expression was highly variable and not normally distributed in either group of HASMC lines. Violin plots showed that the N-HASMC lines distributed into two clusters representing higher and lower-expressors (Fig. 4B). In contrast, only a few SA-HASMC lines had comparably high sGCβ1 expression and most distributed into lower ranges, with seven lines showing very low levels. The mean level of sGCβ1 expression in the SA-HASMC lines was only 60% that in the N-HASMC lines (Fig. 4C). We also observed variability for sGCβ1 expression in lung tissue samples and the expression levels were less in the tissues from severe asthmatics (Fig. S3). In contrast to sGCβ1, the expression levels of sGCα1 and hsp90 were more tightly distributed and less variable in both groups of HASMC, although 7 SA-HASMC lines showed a modestly-diminished level of hsp90 expression (Fig. 4A and B). There was no correlation between the expression levels of sGCβ1 and the levels of either hsp90 or sGCα1 in the HASMC lines (Fig. S5). Despite this finding, there appeared to be some variability in hsp90 expression in the human lung tissue samples and perhaps some correlation with the sGCβ1 expression (Fig. S3).

PDE5A expression in both groups of HASMC was variable and somewhat lower in the SA-HASMC lines (Fig. 4 A-C). This means that increased PDE5A expression was not present in the HASMC lines, and therefore not likely to negatively impact their NO-sGC-cGMP signaling. This may distinguish severe asthma from other pulmonary diseases where elevated PDE5A expression is often present and likely compromises NO-sGC-cGMP signaling [29]. We also found that PKG-1 was expressed in all the N-HASMC and the SA-HASMC lines, with only three of the sixteen N-HASMC lines showing a partly diminshed expression level (Fig. 4A–C). This implies that PKG-1 is avaliable to respond to cGMP and promote downstream functions like smooth muscle relaxation and bronchodilation [30].

Together our findings show that the sGCβ1 expression level in cultured HASMC lines and lung tissues was more variable than was their expression of sGCα1 or hsp90, and that the HASMC and lung tissues from severe asthmatics often had lower levels of sGCβ1 expression.

Three redox enzymes that support sGC function show lower expression levels in severe asthma: Several redox enzymes support sGC function in cells and tissues: CYB5R3 maintains the sGC heme in its ferrous state [31,32], while Trx1 and catalase diminish cell oxidative stress and can protect sGC against oxidative inactivation [33,34]. We thus investigated whether lower expression levels of one or more of these support enzymes might correlate with dysfunctional sGC being present in the SA-HASMC lines.

Expression profiling showed that CYB5R3 levels varied widely in the SA-HASMC and N-HASMC lines (Fig. 4A and B, Table S3), with CYB5R3 expression trending lower in the SA-HASMC lines such that their average level was 59% of the N-HASMC group (Fig. 4C). Notably, the levels of CYB5R3 expression correlated well with the levels of sGCβ1 expression in the HASMC (Fig. 4D and Fig. S3, respectively), as has been observed previously for these two proteins in rat aortic smooth muscle cells [32].

Catalase expression was nearly invariant among the N-HASMC lines, but was quite variable among the SA-HASMC lines, with nine showing very low levels (Fig. 4A–C, Table S3). On average the SA-HASMC group catalase expression was only 45% of the N-HASMC group (Fig. 4C). Catalase expression levels also correlated with the cell catalase activities as measured in the supernatants (Fig. 4E and F). We also observed lower catalase expression in lung tissue samples from severe asthma donors,

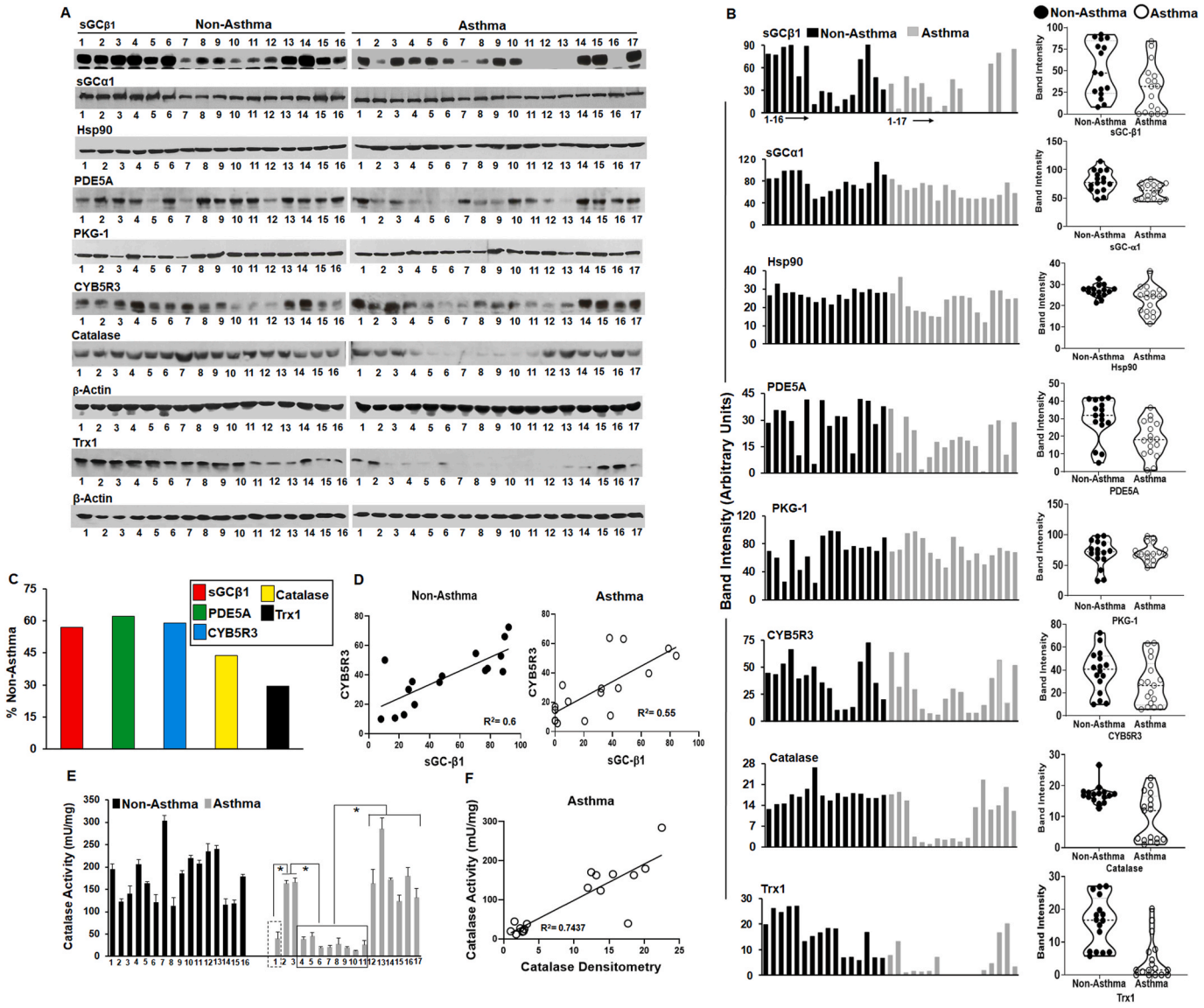

Fig. 4. Relative protein expression levels of the sGC subunits, Hsp90, PDE5A, PKG-1, and three relevant redox enzymes in the normal and severe asthmatic HASMC. Supernatants from 16 non-asthma and 17 severe asthma HASMC lines were run on SDS-PAGE and subject to Western analysis to determine and compare the expression levels of the indicated proteins. (A) Representative Western blots for samples run on 8% SDS-PAGE (top seven proteins) or 15% SDS-PAGE (bottom two proteins). For each protein of interest, equal total supernatant protein was run for each normal and severe asthma HASMC, and the gels underwent Western transfer and all subsequent procedures together for consistency and to allow a direct comparison of the band intensities across all the HASMC samples for each given protein of interest. (B) Left, bar graphs show the mean relative protein expression levels (n = 2 repeats) in normal and severe asthmatic HASMC supernatants, calculated from the band intensities as depicted in Panel A after they each were normalized to their corresponding β-actin band intensity. Right, corresponding violin plots that show the relative distribution of each protein's expression level in the two groups of HASMC. (C) The average expression levels of the designated proteins in the severe asthma HASMC group relative to the normal HASMC group. (D) Correlation between the CYB5R3 and sGCβ1 protein expression levels in the normal and severe asthma HASMC lines. (E) Catalase activities in the non-asthma and severe asthma HASMC supernatants. Activities are the mean (n = 3 repeats per condition) ± SD. *$p < 0.05$, by one-way ANOVA. (F) Relationship between the levels of catalase protein expression and the catalase activities in the severe asthma HASMC. In Panels D and F, lines of best fit are shown along with correlation coefficients.

and among individual donors their tissue expression level matched what was seen in their HASMC (Fig. S4). Unlike for CYB5R3, there was no correlation between the catalase and sGCβ1 expression levels in the HASMC (Fig. S5).

Trx1 expression varied in both groups of HASMC (Fig. 4 A & B, tabulated in Table S3). The N-HASMC lines distributed into three equally-populated groups, while a majority of the SA-HASMC lines distributed into a group with very low Trx1 expression (Fig. 4 A & B). This dropped the average Trx1 expression level in SA-HASMC to 30% that of the N-HASMC lines (Fig. 4C). Lung tissue samples from severe asthma donors also had lower Trx1 expression levels which correlated with lower levels being present in the HASMC derived from the same individual donors (Fig. S4). Again, unlike for CYB5R3, the Trx1 and sGCβ1 expression levels did not correlate in the HASMC lines (Fig. S5).

Overall, our findings reveal that many HASMC lines and lung tissues from severe asthmatics expressed lower levels of three enzymes that support sGC function (CYB5R3, catalase, and Trx1), with CYB5R3 being distinguished by its expression being correlated with the level of sGCβ1 expression in the HASMC lines and in the lung tissue samples.

Low CYB5R3 expression is associated with sGC dysfunction: We next examined if sGC dysregulation in the HASMC would be related to the different expression levels of CYB5R3. We found that low levels of

CYB5R3 expression correlated strongly with the cells having an aberrant sGC activation response, as indicated by poor BAY-41 activation and stronger activation by BAY-60 (Fig. 5A and B), and with their having a low proportion of sGC in its heterodimer form (Fig. 5C). Remarkably, dysfunctional sGC activation was invariantly present in ten HASMC lines whose CYB5R3 expression fell below a certain threshold level (Fig. 5A, dashed line). Among these ten, seven were SA-HASMC lines and three were N-HASMC lines, and they clustered together in the lower portion of the violin plot of Fig. 5B, with the violin inflections indicating the approximate threshold level for effective CYB5R3 expression. A similar threshold expression level was required for sGC heterodimer formation, with a few exceptions (Fig. 5C).

Low catalase an Trx1 expression levels are also associated with sGC dysfunction: Of the eight SA-HASMC lines that showed low catalase expression, six displayed aberrant sGC activation (Fig. 6A and S4). Similarily, of the eight SA-HASMC lines with very low levels of Trx1 expression, six displayed an aberrant sGC activation response (Fig. 6B). These data suggest that there may be threshold levels of catalase and TRx1 expression below which sGC is adversely affected.

Together, our results indicate that a low level of CYB5R3 expression correlated most strongly and with a dysfunctional sGC in the SA-HASMC and N-HASMC lines. Low levels of catalase and Trx1 expression also occurred more often in the SA-HASMC lines and correlated with dysfunctional sGC, although not invariably.

An increased expression of heme catabolism enzymes in severe asthma: Cellular heme must be provided to sGC in order for it to mature into an NO-responsive enzyme [35,36]. Heme oxygenases 1 and 2 (HO1 and HO2) are present in the cell to regulate cellular heme levels by catabolizing heme to biliverdin and CO [37,38]. Most of the SA-HASMC lines showed an increased HO1 expression level that on average was ~2.5 times higher compared to the N-HASMC lines (Fig. 7A and B, Table S3). HO2 expression was also higher in most of the SA-HASMC lines (Fig. 7A and B, Table S3). There was little to no correlation between the HO1, HO2, or sGCβ1 expression levels (Fig. S5). The SA-HASMC lines with higher HO2 expression levels were more prone to have an aberrant sGC activation response (Fig. 7C). Together, our data show that the majority of the SA-HASMC lines have increased HO1 and HO2 expression levels that for in the case of HO2 may correlate with greater sGC dysfunction.

A mouse model of allergen-induced asthma causes change in lung protein expression levels that partly mimic those present in the SA-HASMC lines: Because airway sGC dysfunction also develops in allergen-challenged mice [11], we examined if the proteins we studied change their expression levels upon allergen-challenge. In lung tissue samples from mice that had undergone a house dust mite-challenge protocol, we observed an increased expression of HO1 and HO2 and a decreased expression of Trx1, and no considerable change in the catalase or sGCβ1 expression levels (Fig. S6). Thus, *in situ* changes in the HO1, HO2, and Trx1 expression levels that were brought on by the allergen challenge in mice matched the expression changes that we observed to be inherently present in most of the SA-HASMC lines.

4. Discussion

We found that a majority of HASMC derived from severe asthma donors express an sGC that is primarily or completely unresponsive toward NO, making them dysfunctional for NO-sGC-cGMP signaling. Notably, these SA-HASMC harbored their dysfunctional sGC after being isolated from the lung and passaged three to six times in culture. This argues that their sGC defect is an inherent and stable feature and is not attributable to *in situ* environmental factors present in the inflamed lung that can disable sGC. Notably, lung tissue samples we obtained from the severe asthma donors also displayed levels of sGC dysfunction and altered protein expression patterns that matched with what we observed in the corresponding isolated SA-HASMC. This apparent equivalence is important for two reasons: First, it suggests that the sGC dysfunction and altered protein expression patterns that we observed in many of the SA-HASMC lines were not an artifact of their being isolated from the lung and cultured *in vitro*. Second, because several other lung cell types express sGC, it suggests that the sGC dysfunction may not limited to the HASMC and instead might be systemic within the lung or even possibly throughout the body. These concepts have potentially important biomedical implications and should be further explored. At present, our findings provide a first indication that sGC dysfunction can be inherent and can be found to cluster within a human disease subpopulation, in this case clustering in severe asthmatics.

In human airways, activating the NO-sGC-cGMP pathway promotes a level of bronchodilation that is equivalent to what is achieved by activating the β_2-agonist-cAMP signaling pathway [12]. Our data showed that one of these two bronchodilation pathways (i.e., NO-sGC-cGMP) was often dysfunctional in the severe asthmatic donors. Whether this defect alone would be enough to impact their airway function or to predispose them toward severe asthma is a medically important question, but currently unclear. Of note, an unbiased information mining study by Schmidt and colleagues [39] found that an aberrant sGC activation response is linked to an increased risk of asthma in humans. These potential links between sGC dysfunction and asthma as indicated by their information study and by our current results have fundamental implications for the disease pathogenesis and treatment of asthma, and should be investigated.

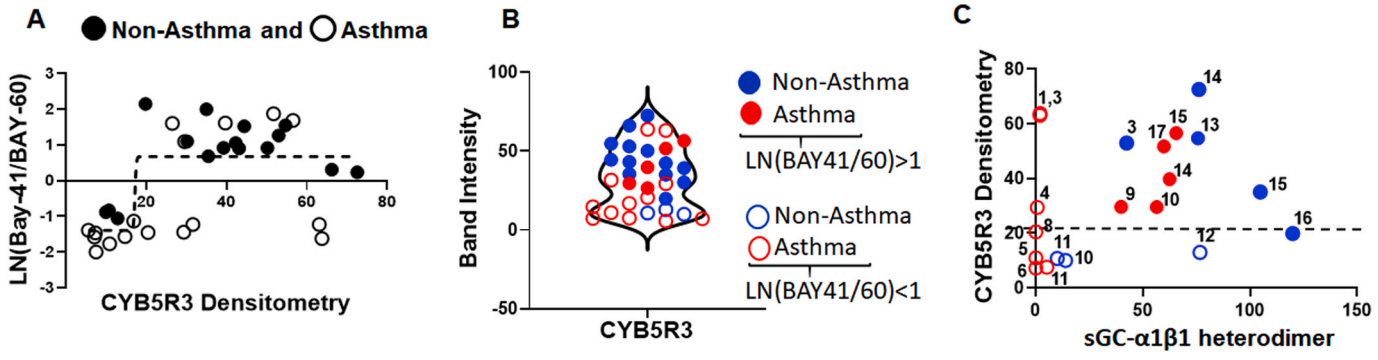

Fig. 5. Relationship between the level of CYB5R3 expression and the sGC activation response profile and heterodimer content in HASMC. (A) Distribution of the HASMC lines regarding their sGC activation response profiles (natural log of the BAY-41/BAY-60 activation ratio) in relation to their expression levels of CYB5R3. Values were calculated from data in Figs. 1 and 4. (B) Violin plot distribution of the HASMC lines according to their CYB5R3 protein densitometries from panel A, with the sGC cell group identity and activation response ratio color-coded as indicated. (C) CYB5R3 expression levels in relation to the relative sGC heterodimer levels for the indicated HASMC lines, whose cell group and activation responses are color-coded as in panel B. HASMC lines depicted and numbered in panel C are the same lines as those analyzed in Fig. 2. (For interpretation of the references to color in this figure legend, the reader is referred to the Web version of this article.)

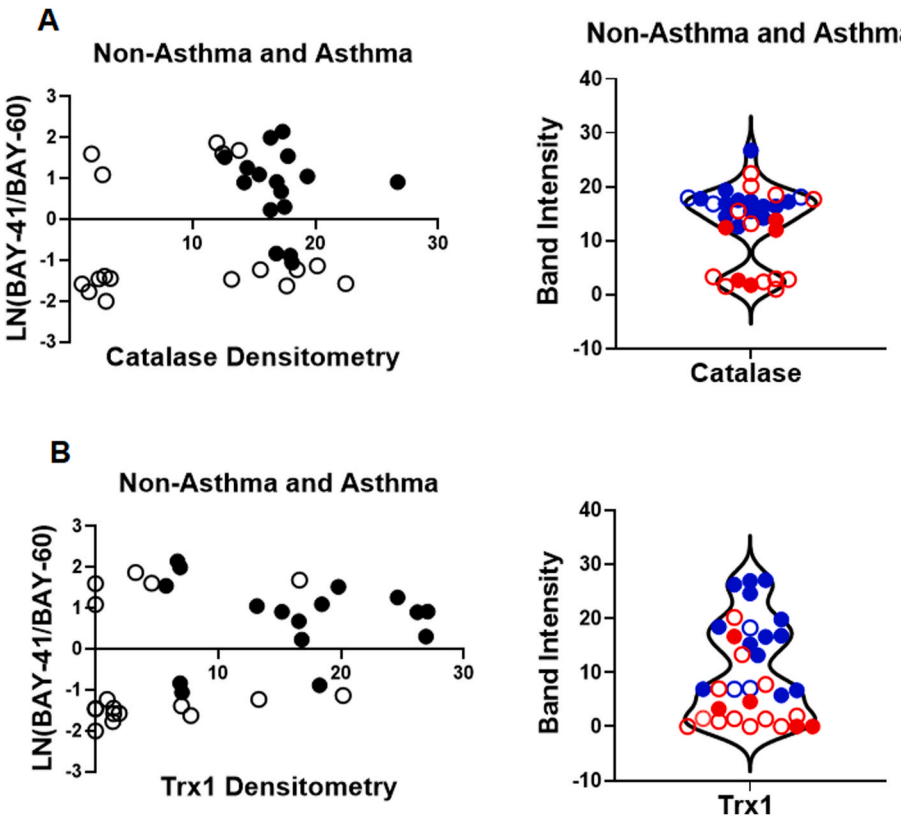

Fig. 6. Relationship between the sGC activation response profile of the HASMC and their Catalase or Trx1 protein expression levels. (A and B) The left-most panels show the distribution of the non-asthma (solid circles) and asthma (open circles) HAMC lines regarding their sGC activation response profiles (natural log of the BAY-41/BAY-60 activation ratio) and their expression level of each protein. Values were calculated from data in Figs. 1 and 4. The right-most panels show the violin plot distribution of the HASMC lines regarding their protein densitometries with sGC activation responses also indicated. Non-asthma (blue), asthma (red), closed circles LN (BAY-41/BAY-60) $>$ 1, open circles LN(BAY-41/BAY-60) $<$ 1. (For interpretation of the references to color in this figure legend, the reader is referred to the Web version of this article.)

Our molecular studies shed light on the nature of the sGC defect in the SA-HASMC and its possible mechanisms. In almost all cases, the aberrant sGC activation response in the SA-HASMC (NO-insensitivity and higher BAY-60 activation) correlated with their having a lower amount of sGC in heterodimer form and with more of the sGCβ1 subunit being complexed instead with hsp90. Previous studies indicate that this situation can arise in cells or in tissues when the sGC heterodimer undergoes redox damage or when heme is unavailable to the sGCβ1 subunit during its maturation [11,21,22]. Damage to the sGC heterodimer takes place in cells or tissues upon exposure to excessive NO or reactive oxygen species [11,40–42]. Although studies indicate that greater oxidative stress exists in the asthmatic airway [33,34], it is unclear if this condition remains inherent in the isolated SA-HASMC themselves and would persist after their isolation. This deserves further investigation. Buildup of heme-free sGCβ1 could occur if the SA-HASMC have a dysfunctional heme biosynthesis or transport mechanism [43] or if they have imbalanced rates of heme biosynthesis and catabolism by HO enzymes [44]. Whether any of these scenarios play out within the individual SA-HASMC lines is an important follow-up question that can now be addressed, as guided by our findings on the redox and other proteins that we examined.

CYB5R3 supports NO-responsive sGC by reducing its ferric heme to ferrous [32]. When CYB5R3 expression was knocked down in cells or in mice, their sGC became more susceptible to oxidative stressors causing NO-insensitivity and led to a greater BAY-60 activation response [45]. In our study, we found a strong correlation exists between low levels of CYB5R3 expression and sGC dysfunction in the HASMC lines and lung tissues. For example, all eight SA-HASMC lines that show low levels of CYB5R3 expression invariably contained an NO-insensitive sGC (Table S3). Of the 16 N-HASMC lines that we studied, only four were seen to have a low CYB5R3 expression level, and three of these four have a dysfunctional sGC, and are the only N-HASMC lines that do so (Table S3). Finally, of the nine SA-HASMC lines that show a normal level of CYB5R3 expression, five contain a NO-responsive sGC that is primarily heterodimeric, and these five are the only SA-HASMC lines that do so (Table S3). We also saw that HASMC that have low levels of CYB5R3 expression had reduced levels of sGCβ1 protein expression. This matches findings from a previous study on rat aoertic smooth muscle cells [32], and is consistent with the possibility that sGCβ1 may become more susceptible to degradation when its heme becomes oxidized [26,46]. Whether HASMC need to maintain a sufficient level of CYB5R3 activity in order to stabilize the sGCβ1 protein deserves further study. Overall, our findings reveal that CYB5R3 plays a key role in the expression of an NO-reponsive sGC heterodimer in HASMC, and when the CYB5R3 expression level falls below a certain threshold, it is strongly associated with sGC dysfunction.

Oxidative stress can damage sGC in tissues [26,47–49] and this circumstance prevails in asthmatic airways due to higher oxidant production and decreased antioxidant defense, including lower catalase activity [33,34]. Inhibiting Trx1 or its cognate reductase also promotes formation of dysfunctional sGC in cells [42,50]. We found that most SA-HASMC lines have a low Trx1 expression level and half have very low catalase expression as well. This circumstance likely increases the oxidant stress level within the SA-HASMC, which in turn would be conducive for sGC damage and development of NO insensitivity. However, our data suggest that low catalase or Trx1 expression, on their own or together, did not invariably render sGC dysfunctional in the SA-HASMC lines (Table S3). Despite this, it remains possible that their lower Trx1 and catalase expression levels sensitize their sGC to become dysfunctional when they exist within the inflammatory asthmatic airway. This possibility can now be addressed.

We also found higher than normal HO1 and HO2 expression levels in most of the SA-HASMC lines. Increasing HO1 expression in cells or tissues was reported to cause sGC to become NO-unresponsive and to be activated by BAY-60 to a greater extent [51,52]. This circumstance could arise if the excess HO1 expression decreased the level of intracellular heme that is available during sGC maturation. The lung HO1 expression level also increased in animal models of inflammatory

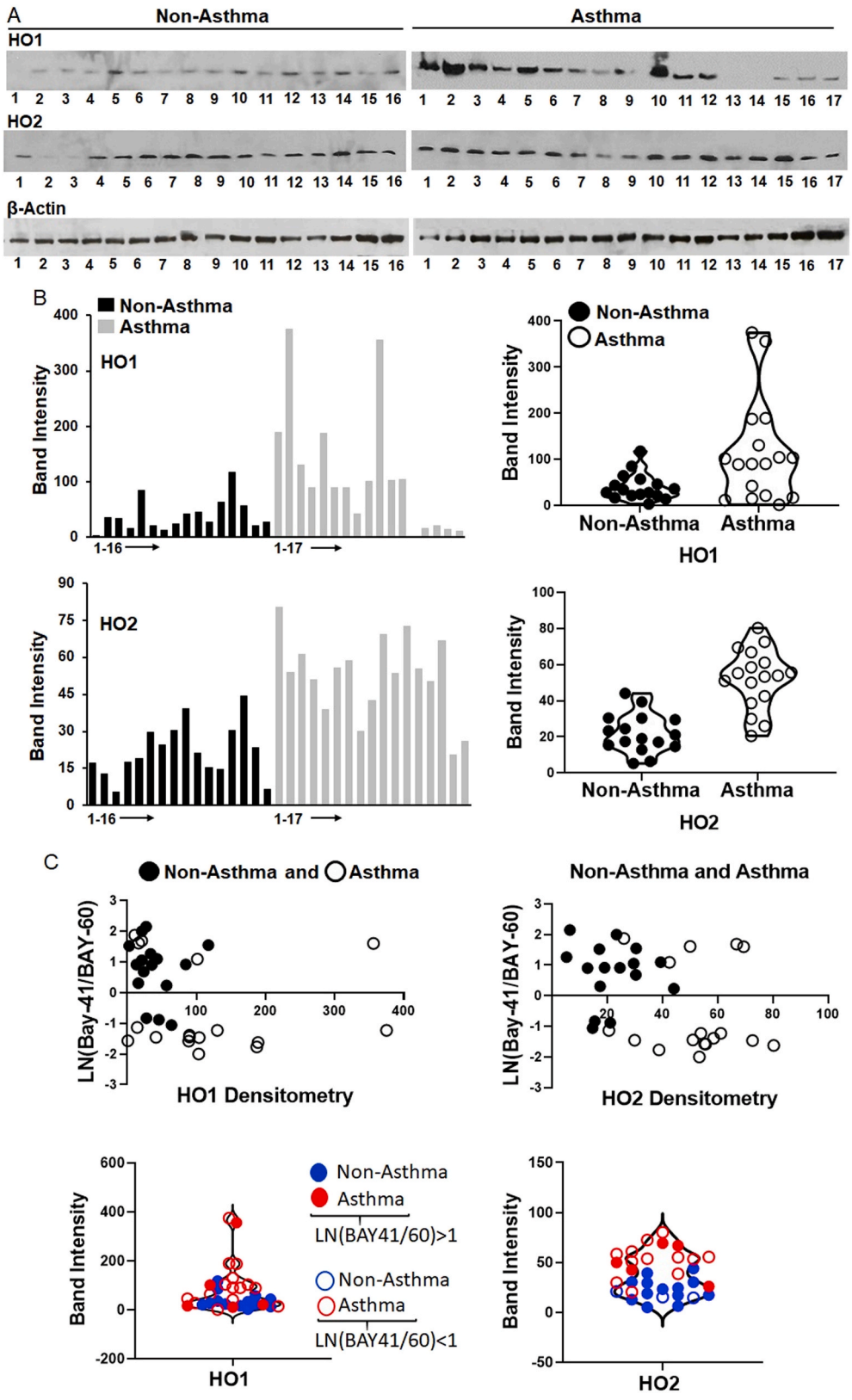

Fig. 7. HO1 and HO2 expression levels in non-asthma and severe asthma HASMC lines and their relationship to their sGC activation response profiles. (A) Representative Western blots showing the relative expression levels of HO1 and HO2. (B) Left: Mean densitometry measures of HO1 and HO2 bands (n = 2 repeats, normalized to β-actin band intensities) calculated from results as in Panel A. Right: Violin plots of the mean densitometry data showing the distribution of HO1 and HO2 expression among the HASMC lines. (C) Relationship between the sGC activation response profiles (the natural log of the BAY-41/BAY-60 activation ratio, calculated from data in Fig. 1) and the levels of HO1 and HO2 expression in each HASMC line. The lower panels show the violin plot distribution of the HASMC lines regarding their HO1 and HO2 protein expression, with their individual sGC activation response ratios color-coded as indicated. (For interpretation of the references to color in this figure legend, the reader is referred to the Web version of this article.)

asthma [53] (Fig. S6), where sGC also becomes NO-unresponsive [11]. In our current study, higher HO1 or HO2 expression levels were not invariably associated with sGC dysfunction (Table S3). Again, it is plausible that higher HO1 and HO2 expression levels could create an underlying heme deficit that predisposesthe SA-HASMC to express more heme-free sGCβ1, particularly if the cells possess other defects or are oxidatively stressed in the inflamed asthmatic airway.

Our results from the allergen-induced mouse model confirm reports that protein expression patterns do change in the lung and in HASMC as a consequence of airway inflammation [54,55]. Potentially, these *in situ* changes would add another layer of complexity in understanding asthma pathogenesis. However, note that we found similarity between

the SA-HASMC and lung tissue derived from the same donors regarding their sGC activation profiles or protein expression patterns. This implies that being in the lung environment did not drastically alter the sGC phenotype or protein expression pattern in the HASMC, at least for the small number of donors that we were able to compare in this way.

Fig. 8 depicts a model that summarizes our current findings in the context of what is known about sGC maturation, function, and dysregulation leading to compromised NO-sGC-cGMP signaling. As shown on the left, during the maturation process GAPDH delivers heme to an apo-sGCβ1 subunit that is in complex with hsp90 [36]. If higher levels of HO1 and HO2 expression diminish the available intracellular heme it may inhibit heme delivery to sGCβ1, which would cause the cell to build up relatively higher levels of the sGCβ1-hsp90 complex and diminish the extent of sGC heterodimer formation. However, in this circumstance BAY-60 is able to bind in the apo-sGCβ1-hsp90 complex and drive it to form of an active sGC heterodimer [21]. If heme becomes inserted into sGCβ1, hsp90 dissociates and sGCβ1 binds with an sGCα1 subunit to create the sGC heterodimer [21] that can respond to NO and function normally in NO-sGC-cGMP signaling. The ferrous heme in the sGC heterodimer is kept reduced by CYB5R3 [32] so that sGC can respond to NO and activate its cGMP production. When the CYB5R3 expression level falls too low it makes the sGC heme more susceptible to oxidation and to developing NO insensitivity and heterodimer breakup. This may additionally lead to enanced degradation of the sGCβ1 subunit. The actions of catalase and Trx1 can help to shield sGC protein components from oxidation, and their lower expression levels sensitize sGC to protein or heme oxidation events that lead to disruption of the sGC heterodimer and the reassociation of the sGCβ1 subunit with hsp90.

It is important to note that dysfunctional sGC could also arise in HASMC that harbor possible defects that we did not study here. For example, there could be genetic modifications in the sGC subunits that predispose a poor heterodimer formation and dysfunctional sGC. Possible examples of this are the SA-HASMC lines 1 and 3, which have extremely poor sGC heterodimer formation despite having a high expression level of CYB5R3 (see Fig. 5C). Such mechanisms would act distinct from or in addition to those presented in Fig. 8.

Conclusions and future directions: Working with HASMC from individual donors provides a unique platform to explore the heterogeneity of airway disease etiology. Despite the inherent heterogeneity, our data uncover a clear clustering of sGC dysfunction in the HASMC of severe asthmatics, and its close correlation with a poor CYB5R3 expression and divergent expression of other redox enzymes that impact sGC. Indeed, it is evident that sGC dysfunction is a common feature among the SA-HASMC lines and is associated with patterns of support protein expression that significantly differ relative to the N-HASMC lines (Table S3). It will now be important to test if correcting the abbarent protein expression levels in individual SA-HASMC lines, for example by increasing the expression level of CYB5R3, catalase, or Trx1, or by governing HO1 and HO2 expression and intracellular heme availability, alone or in combinations, can restore sGC function and NO sensitivity. If such modifications rescue the sGC phenotype then the findings may be further translated to help guide potential therapeutic approaches. It is also important to mention that severe asthma patients harboring an NO-unresponsive sGC might still be effectively treated by drugs that mimic BAY-60 in directly activating the NO-unresponsive sGC. Although no drugs of this type are currently available for human use, a few are in clinical trials to explore their efficacy in other diseases [56]. This strategy may be particularly beneficial in light of our finding normal ranges of PDE5 and PKG-1 expression among the SA-HASMC lines, which indicates that the cGMP-dependent and PKG-1-based bronchodilation pathway is generally available in severe asthmatics. Overall, our finding that inherent sGC dysfunction is relatively common in the severe asthmatic airway places a new emphasis on NO-sGC-cGMP signaling that may ultimately help to understand the disease and guide therapeutic interventions.

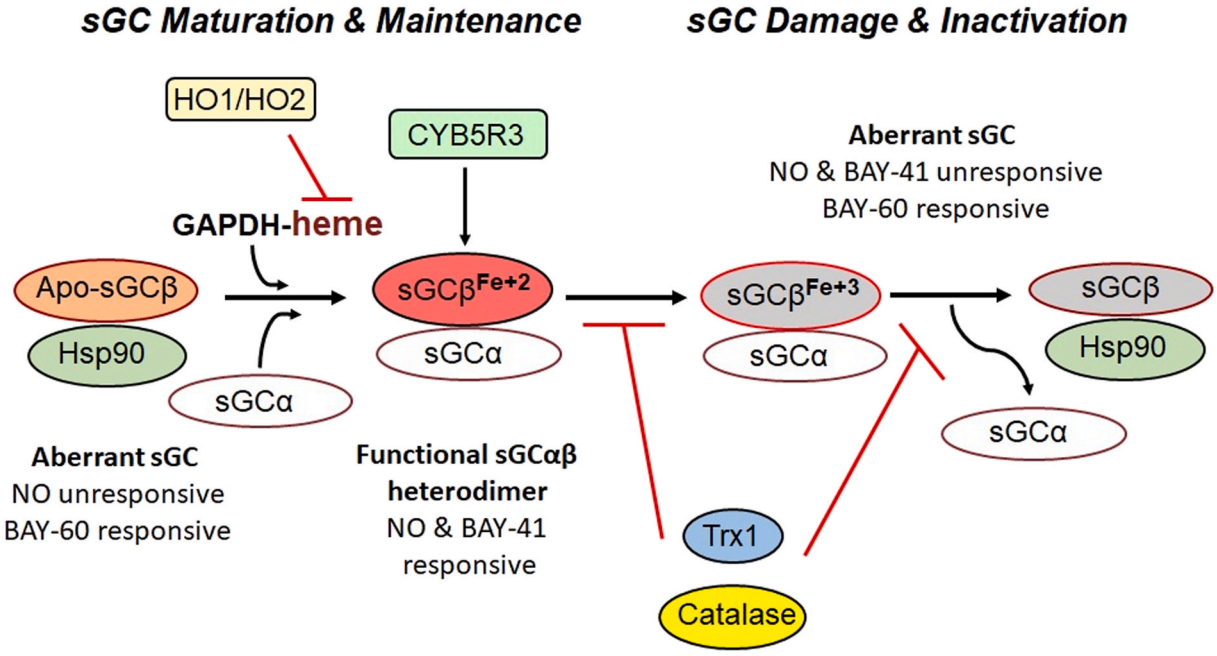

Fig. 8. Model of sGC maturation and inactivation and how HO1, HO2, CYB5R3, Trx1, and catalase may impact these processes. During maturation the apo-sGCβ1 subunit is in complex with hsp90 and receives heme from GAPDH. Higher levels of HO1 and HO2 expression in the severe asthmatic HASMC may diminish intracellular heme and compromise heme delivery to sGCβ. Once heme is inserted into sGCβ it dissociates hsp90 and binds with a sGCα subunit to create the functional and NO-responsive sGC heterodimer. CYB5R3 keeps the sGC heme reduced in ferrous form so that it can be activated by NO for cGMP production. Low levels of CYB5R3 expression in the severe asthmatic HASMC make the sGC ferrous heme more susceptible to oxidation to its ferric form, which creates NO insensitivity, and leads to heterodimer dissociation. Trx1 and catalase help to protect sGC protein components from oxidation. Their lower expression levels in the severe asthmatic HASMC may sensitize sGC to oxidation and lead to the breakup of the heterodimer and reassociation of the sGCβ subunit with hsp90. The status of the sGCαβ heterodimer and its heme determines the pharmacophore response to NO or BAY-41 *versus* BAY-60.

Author contributions

A. Ghosh and D. J. Stuehr designed the experiments. W. F. Jester, C. K. White, and R. Panettieri generated the HASMC lines and lung tissue samples. K. Asosingh supplied murine asthma model mouse lung tissues for biochemical measures. A. Ghosh performed all the cell culture and biochemical studies. A. Ghosh, D. J. Stuehr, R.A. Panettieri, S.C. Erzurum, and C.K. White analyzed the data. A. Ghosh and D. J. Stuehr wrote the manuscript.

Declaration of competing interest

The authors declare no conflict of interest.

Acknowledgements

This work was supported by National Institutes of Health Grants (National Heart, Lung, And Blood Institute), U.S.A., R56HL139564, R01HL150049 (A.G.) and P01HL081064 (S.C.E., D.J.S., R.A.P., K.A. and A.G.).

Abbreviations

BAY-41 BAY 41-2272
BAY-60 BAY 60-2770
HDME House dust mite extract
N-HASMC Non-Asthma Human airway smooth muscle cell
SA-HASMC Severe-asthma Human airway smooth muscle cell

Appendix A. Supplementary data

Supplementary data to this article can be found online at https://doi.org/10.1016/j.redox.2020.101832.

References

[1] S.T. Holgate, S. Wenzel, D.S. Postma, S.T. Weiss, H. Renz, P.D. Sly, Epub 2015/01/01, Asthma. Nat Rev Dis Primers. 1 (2015) 15025, https://doi.org/10.1038/nrdp.2015.25. PubMed PMID: 27189668; PMCID: PMC7096989.
[2] C. Nunes, A.M. Pereira, M. Morais-Almeida, Asthma costs and social impact, Epub 2017/01/13, Asthma Res Pract 3 (2017) 1, https://doi.org/10.1186/s40733-016-0029-3. PubMed PMID: 28078100; PMCID: PMC5219738.
[3] K.F. Chung, S.E. Wenzel, J.L. Brozek, A. Bush, M. Castro, P.J. Sterk, I.M. Adcock, E. D. Bateman, E.H. Bel, E.R. Bleecker, L.P. Boulet, C. Brightling, P. Chanez, S. E. Dahlen, R. Djukanovic, U. Frey, M. Gaga, P. Gibson, Q. Hamid, N.N. Jajour, T. Mauad, R.L. Sorkness, W.G. Teague, International ERS/ATS guidelines on definition, evaluation and treatment of severe asthma, Epub 2013/12/18, Eur. Respir. J. 43 (2) (2014) 343–373, https://doi.org/10.1183/09031936.00202013. PubMed PMID: 24337046.
[4] R. Hartley, R. Berair, C.E. Brightling, Severe asthma: novel advances in the pathogenesis and therapy, Epub 2014/05/02, Pol. Arch. Med. Wewn. 124 (5) (2014) 247–254, https://doi.org/10.20452/pamw.2253. PubMed PMID: 24781552.
[5] B.N. Lambrecht, H. Hammad, The airway epithelium in asthma, Epub 2012/05/09, Nat. Med. 18 (5) (2012) 684–692, https://doi.org/10.1038/nm.2737. PubMed PMID: 22561832.
[6] Y.S. Prakash, Emerging concepts in smooth muscle contributions to airway structure and function: implications for health and disease, Epub 2016/10/16, Am. J. Physiol. Lung Cell Mol. Physiol. 311 (6) (2016) L1113–L1140, https://doi.org/10.1152/ajplung.00370.2016. PubMed PMID: 27742732; PMCID: PMC5206394.
[7] R.J. Russell, C. Brightling, Pathogenesis of asthma: implications for precision medicine, Epub 2017/07/02, Clin. Sci. (Lond.) 131 (14) (2017) 1723–1735, https://doi.org/10.1042/CS20160253. PubMed PMID: 28667070.
[8] M.M. Stein, E.E. Thompson, N. Schoettler, B.A. Helling, K.M. Magnaye, C. Stanhope, C. Igartua, A. Morin, C. Washington 3rd, D. Nicolae, K. Bonnelykke, C. Ober, A decade of research on the 17q12-21 asthma locus: piecing together the puzzle, e3. Epub 2018/01/09, J. Allergy Clin. Immunol. 142 (3) (2018) 749–764, https://doi.org/10.1016/j.jaci.2017.12.974. PubMed PMID: 29307657; PMCID: PMC6172038.
[9] 2013 D.C. Doeing, J. Solway, Airway smooth muscle in the pathophysiology and treatment of asthma, Epub 2013/01/12, J. Appl. Physiol. 114 (7) (1985) 834–843, https://doi.org/10.1152/japplphysiol.00950.2012. PubMed PMID: 23305987; PMCID: PMC3633438.
[10] C.K. Billington, O.O. Ojo, R.B. Penn, S. Ito, cAMP regulation of airway smooth muscle function, Epub 2012/05/29, Pulm. Pharmacol. Therapeut. 26 (1) (2013) 112–120, https://doi.org/10.1016/j.pupt.2012.05.007. PubMed PMID: 22634112; PMCID: PMC3574867.
[11] A. Ghosh, C.J. Koziol-White, K. Asosingh, G. Cheng, L. Ruple, D. Groneberg, A. Friebe, S.A. Comhair, J.P. Stasch, R.A. Panettieri Jr., M.A. Aronica, S. C. Erzurum, D.J. Stuehr, Soluble guanylate cyclase as an alternative target for bronchodilator therapy in asthma, Epub 2016/04/14, Proc. Natl. Acad. Sci. U. S. A. 113 (17) (2016) E2355–E2362, https://doi.org/10.1073/pnas.1524398113. PubMed PMID: 27071111; PMCID: PMC4855555.
[12] C.J. Koziol-White, A. Ghosh, P. Sandner, S.E. Erzurum, D.J. Stuehr, R. A. Panettieri Jr., Soluble guanylate cyclase agonists induce bronchodilation in human small airways, Epub 2019/07/25, Am. J. Respir. Cell Mol. Biol. 62 (1) (2020) 43–48, https://doi.org/10.1165/rcmb.2019-0001OC. PubMed PMID: 31340135; PMCID: PMC6938135.
[13] E.J. Tsai, D.A. Kass, Cyclic GMP signaling in cardiovascular pathophysiology and therapeutics, Epub 2009/03/25, Pharmacol. Ther. 122 (3) (2009) 216–238, https://doi.org/10.1016/j.pharmthera.2009.02.009. PubMed PMID: 19306895; PMCID: PMC2709600.
[14] E. Buys, P. Sips, New insights into the role of soluble guanylate cyclase in blood pressure regulation, Epub 2014/01/15, Curr. Opin. Nephrol. Hypertens. 23 (2) (2014) 135–142, https://doi.org/10.1097/01.mnh.0000441048.91041.3a. PubMed PMID: 24419369; PMCID: PMC4102174.
[15] J.P. Stasch, P. Pacher, O.V. Evgenov, Soluble guanylate cyclase as an emerging therapeutic target in cardiopulmonary disease, Epub 2011/05/25, Circulation 123 (20) (2011) 2263–2273, https://doi.org/10.1161/CIRCULATIONAHA.110.981738. PubMed PMID: 21606405; PMCID: PMC3103045.
[16] A.M. Hamad, A. Clayton, B. Islam, A.J. Knox, Guanylyl cyclases, nitric oxide, natriuretic peptides, and airway smooth muscle function, Epub 2003/10/11, Am. J. Physiol. Lung Cell Mol. Physiol. 285 (5) (2003) L973–L983, https://doi.org/10.1152/ajplung.00033.2003. PubMed PMID: 14551038.
[17] M. Lam, J.E. Bourke, A new pathway to airway relaxation: targeting the "other" cyclase in asthma, Epub 2019/08/16, Am. J. Respir. Cell Mol. Biol. 62 (1) (2020) 3–4, https://doi.org/10.1165/rcmb.2019-0274ED. PubMed PMID: 31414885; PMCID: PMC6938138.
[18] M.K. Gupta, K. Asosingh, M. Aronica, S. Comhair, G. Cao, S. Erzurum, R. A. Panettieri Jr., S.V. Naga Prasad, Defective resensitization in human airway smooth muscle cells evokes beta-adrenergic receptor dysfunction in severe asthma, Epub 2015/05/30, PloS One 10 (5) (2015), e0125803, https://doi.org/10.1371/journal.pone.0125803. PubMed PMID: 26023787; PMCID: PMC4449172.
[19] M. Kabesch, J. Tost, Recent findings in the genetics and epigenetics of asthma and allergy, Epub 2020/02/16, Semin. Immunopathol. 42 (1) (2020) 43–60, https://doi.org/10.1007/s00281-019-00777-w. PubMed PMID: 32060620; PMCID: PMC7066293.
[20] P.G. Woodruff, Gene expression in asthmatic airway smooth muscle, Epub 2007/12/21, Proc. Am. Thorac. Soc. 5 (1) (2008) 113–118, https://doi.org/10.1513/pats.200705-059VS. PubMed PMID: 18094093; PMCID: PMC2645297.
[21] A. Ghosh, J.P. Stasch, A. Papapetropoulos, D.J. Stuehr, Nitric oxide and heat shock protein 90 activate soluble guanylate cyclase by driving rapid change in its subunit interactions and heme content, Epub 2014/04/16, J. Biol. Chem. 289 (22) (2014) 15259–15271, https://doi.org/10.1074/jbc.M114.559393. PubMed PMID: 24733395; PMCID: PMC4140884.
[22] A. Ghosh, D.J. Stuehr, Soluble guanylyl cyclase requires heat shock protein 90 for heme insertion during maturation of the NO-active enzyme, Epub 2012/07/28, Proc. Natl. Acad. Sci. U. S. A. 109 (32) (2012) 12998–13003, https://doi.org/10.1073/pnas.1205854109. PubMed PMID: 22837396; PMCID: PMC3420196.
[23] S. Jonasson, G. Hedenstierna, H. Hedenstrom, J. Hjoberg, Comparisons of effects of intravenous and inhaled methacholine on airway physiology in a murine asthma model, Epub 2009/01/13, Respir. Physiol. Neurobiol. 165 (2–3) (2009) 229–236, https://doi.org/10.1016/j.resp.2008.12.005. PubMed PMID: 19136080.
[24] M. Follmann, N. Griebenow, M.G. Hahn, I. Hartung, F.J. Mais, J. Mittendorf, M. Schafer, H. Schirok, J.P. Stasch, F. Stoll, A. Straub, The chemistry and biology of soluble guanylate cyclase stimulators and activators, Epub 2013/08/22, Angew Chem. Int. Ed. Engl. 52 (36) (2013) 9442–9462, https://doi.org/10.1002/anie.201302588. PubMed PMID: 23963798.
[25] F. Theilig, M. Bostanjoglo, H. Pavenstadt, C. Grupp, G. Holland, I. Slosarek, A. M. Gressner, M. Russwurm, D. Koesling, S. Bachmann, Cellular distribution and function of soluble guanylyl cyclase in rat kidney and liver, J. Am. Soc. Nephrol. 12 (11) (2001) 2209–2220. Epub 2001/10/25. PubMed PMID: 11675397.
[26] L.S. Hoffmann, P.M. Schmidt, Y. Keim, S. Schaefer, H.H. Schmidt, J.P. Stasch, Distinct molecular requirements for activation or stabilization of soluble guanylyl cyclase upon haem oxidation-induced degradation, Epub 2009/05/27, Br. J. Pharmacol. 157 (5) (2009) 781–795, https://doi.org/10.1111/j.1476-5381.2009.00263.x. PubMed PMID: 19466990; PMCID: PMC2721263.
[27] D.A. Kass, E. Takimoto, T. Nagayama, H.C. Champion, Phosphodiesterase regulation of nitric oxide signaling, PubMed PMID: 17467673, Cardiovasc. Res. 75 (2) (2007) 303–314, https://doi.org/10.1016/j.cardiores.2007.02.031. Epub 2007/05/01.
[28] 1985 T.M. Lincoln, N. Dey, H. Sellak, Invited review: cGMP-dependent protein kinase signaling mechanisms in smooth muscle: from the regulation of tone to gene expression, Epub 2001/08/18, J. Appl. Physiol. 91 (3) (2001) 1421–1430, https://doi.org/10.1152/jappl.2001.91.3.1421. PubMed PMID: 11509544.
[29] J.D. Corbin, A. Beasley, M.A. Blount, S.H. Francis, High lung PDE5: a strong basis for treating pulmonary hypertension with PDE5 inhibitors, Epub 2005/07/19, Biochem. Biophys. Res. Commun. 334 (3) (2005) 930–938, https://doi.org/10.1016/j.bbrc.2005.06.183. PubMed PMID: 16023993.

[30] A. Kovacs, A. Alogna, H. Post, N. Hamdani, Is enhancing cGMP-PKG signalling a promising therapeutic target for heart failure with preserved ejection fraction?, Epub 2016/03/01, Neth. Heart J. 24 (4) (2016) 268–274, https://doi.org/10.1007/s12471-016-0814-x. PubMed PMID: 26924822; PMCID: PMC4796050.
[31] B.G. Durgin, A.C. Straub, Redox control of vascular smooth muscle cell function and plasticity, Epub 2018/02/22, Lab. Invest. 98 (10) (2018) 1254–1262, https://doi.org/10.1038/s41374-018-0032-9. PubMed PMID: 29463879; PMCID: PMC6102093.
[32] M.M. Rahaman, A.T. Nguyen, M.P. Miller, S.A. Hahn, C. Sparacino-Watkins, S. Jobbagy, N.T. Carew, N. Cantu-Medellin, K.C. Wood, C.J. Baty, F.J. Schopfer, E. E. Kelley, M.T. Gladwin, E. Martin, A.C. Straub, Cytochrome b5 reductase 3 modulates soluble guanylate cyclase redox state and cGMP signaling, Epub 2017/06/07, Circ. Res. 121 (2) (2017) 137–148, https://doi.org/10.1161/CIRCRESAHA.117.310705. PubMed PMID: 28584062; PMCID: PMC5527687.
[33] U.M. Sahiner, E. Birben, S. Erzurum, C. Sackesen, O. Kalayci, Oxidative stress in asthma, Epub 2011/10/01, World Allergy Organ J 4 (10) (2011) 151–158, https://doi.org/10.1097/WOX.0b013e318232389e. PubMed PMID: 23268432; PMCID: PMC3488912.
[34] S.A. Comhair, S.C. Erzurum, Redox control of asthma: molecular mechanisms and therapeutic opportunities, Epub 2009/07/29, Antioxidants Redox Signal. 12 (1) (2010) 93–124, https://doi.org/10.1089/ARS.2008.2425. PubMed PMID: 19634987; PMCID: PMC2824520.
[35] A. Ghosh, D.J. Stuehr, Regulation of sGC via hsp90, cellular heme, sGC agonists, and NO: new pathways and clinical perspectives, Antioxidants Redox Signal. 26 (4) (2017) 182–190, https://doi.org/10.1089/ars.2016.6690. PubMed PMID: 26983679; PMCID: PMC5278824.
[36] Y. Dai, E.A. Sweeny, S. Schlanger, A. Ghosh, D.J. Stuehr, GAPDH delivers heme to soluble guanylyl cyclase, Epub 2020/05/03, J. Biol. Chem. 295 (24) (2020) 8145–8154, https://doi.org/10.1074/jbc.RA120.013802. PubMed PMID: 32358060; PMCID: PMC7294094.
[37] D. Morse, A.M. Choi, Heme oxygenase-1: the "emerging molecule" has arrived, Epub 2002/07/02, Am. J. Respir. Cell Mol. Biol. 27 (1) (2002) 8–16, https://doi.org/10.1165/ajrcmb.27.1.4862. PubMed PMID: 12091240.
[38] J. Munoz-Sanchez, M.E. Chanez-Cardenas, A review on hemeoxygenase-2: focus on cellular protection and oxygen response, Epub 2014/08/20, Oxid Med Cell Longev 2014 (2014) 604981, https://doi.org/10.1155/2014/604981. PubMed PMID: 25136403; PMCID: PMC4127239.
[39] F. Langhauser, A.I. Casas, V.T. Dao, E. Guney, J. Menche, E. Geuss, P.W. M. Kleikers, M.G. Lopez, A.L. Barabasi, C. Kleinschnitz, H. Schmidt, A diseasome cluster-based drug repurposing of soluble guanylate cyclase activators from smooth muscle relaxation to direct neuroprotection, Epub 2018/02/10, NPJ Syst Biol Appl 4 (2018) 8, https://doi.org/10.1038/s41540-017-0039-7. PubMed PMID: 29423274; PMCID: PMC5799370 BAY58-2667 and BAY60-2770. The remaining authors declare no competing financial interests.
[40] J. Tejero, S. Shiva, M.T. Gladwin, Sources of vascular nitric oxide and reactive oxygen species and their regulation, Epub 2018/11/01, Physiol. Rev. 99 (1) (2019) 311–379, https://doi.org/10.1152/physrev.00036.2017. PubMed PMID: 30379623; PMCID: PMC6442925.
[41] R.C. Shah, S. Sanker, K.C. Wood, B.G. Durgin, A.C. Straub, Redox regulation of soluble guanylyl cyclase, Epub 2018/03/27, Nitric Oxide 76 (2018) 97–104, https://doi.org/10.1016/j.niox.2018.03.013. PubMed PMID: 29578056; PMCID: PMC5916318.
[42] C. Huang, M. Alapa, P. Shu, N. Nagarajan, C. Wu, J. Sadoshima, V. Kholodovych, H. Li, A. Beuve, Guanylyl cyclase sensitivity to nitric oxide is protected by a thiol oxidation-driven interaction with thioredoxin-1, Epub 2017/07/01, J. Biol. Chem. 292 (35) (2017) 14362–14370, https://doi.org/10.1074/jbc.M117.787390. PubMed PMID: 28659344; PMCID: PMC5582831.
[43] R.K. Donegan, C.M. Moore, D.A. Hanna, A.R. Reddi, Handling heme: the mechanisms underlying the movement of heme within and between cells, Epub 2018/08/10, Free Radic. Biol. Med. 133 (2019) 88–100, https://doi.org/10.1016/j.freeradbiomed.2018.08.005. PubMed PMID: 30092350; PMCID: PMC6363905.
[44] D. Chiabrando, F. Vinchi, V. Fiorito, S. Mercurio, E. Tolosano, Heme in pathophysiology: a matter of scavenging, metabolism and trafficking across cell membranes, Epub 2014/05/02, Front. Pharmacol. 5 (2014) 61, https://doi.org/10.3389/fphar.2014.00061. PubMed PMID: 24782769; PMCID: PMC3986552.
[45] K.C. Wood, B.G. Durgin, H.M. Schmidt, S.A. Hahn, J.J. Baust, T. Bachman, D. A. Vitturi, S. Ghosh, S.F. Ofori-Acquah, A.L. Mora, M.T. Gladwin, A.C. Straub, Smooth muscle cytochrome b5 reductase 3 deficiency accelerates pulmonary hypertension development in sickle cell mice, Epub 2019/12/11, Blood Adv 3 (23) (2019) 4104–4116, https://doi.org/10.1182/bloodadvances.2019000621. PubMed PMID: 31821458; PMCID: PMC6963246.
[46] S. Meurer, S. Pioch, T. Pabst, N. Opitz, P.M. Schmidt, T. Beckhaus, K. Wagner, S. Matt, K. Gegenbauer, S. Geschka, M. Karas, J.P. Stasch, H.H. Schmidt, W. Muller-Esterl, Nitric oxide-independent vasodilator rescues heme-oxidized soluble guanylate cyclase from proteasomal degradation, Epub 2009/05/30, Circ. Res. 105 (1) (2009) 33–41, https://doi.org/10.1161/CIRCRESAHA.109.198234. PubMed PMID: 19478201.
[47] L.S. Hoffmann, P.M. Schmidt, Y. Keim, C. Hoffmann, H.H. Schmidt, J.P. Stasch, Fluorescence dequenching makes haem-free soluble guanylate cyclase detectable in living cells, PloS One 6 (8) (2011), e23596, https://doi.org/10.1371/journal.pone.0023596. PubMed PMID: 21858179; PMCID: PMC3157391.
[48] M. Tawa, T. Okamura, Soluble guanylate cyclase redox state under oxidative stress conditions in isolated monkey coronary arteries, Epub 2016/10/08, Pharmacol Res Perspect 4 (5) (2016), e00261, https://doi.org/10.1002/prp2.261. PubMed PMID: 27713826; PMCID: PMC5045941.
[49] A. Kollau, M. Opelt, G. Wolkart, A.C.F. Gorren, M. Russwurm, D. Koesling, B. Mayer, A. Schrammel, Irreversible activation and stabilization of soluble guanylate cyclase by the protoporphyrin IX mimetic cinaciguat, Epub 2017/11/16, Mol. Pharmacol. 93 (2) (2018) 73–78, https://doi.org/10.1124/mol.117.109918. PubMed PMID: 29138269; PMCID: PMC5916872.
[50] H. Choi, R.C. Tostes, R.C. Webb, Thioredoxin reductase inhibition reduces relaxation by increasing oxidative stress and s-nitrosylation in mouse aorta, Epub 2011/07/29, J. Cardiovasc. Pharmacol. 58 (5) (2011) 522–527, https://doi.org/10.1097/FJC.0b013e31822d80a5. PubMed PMID: 21795991; PMCID: PMC3208795.
[51] T. Imai, T. Morita, T. Shindo, R. Nagai, Y. Yazaki, H. Kurihara, M. Suematsu, S. Katayama, Vascular smooth muscle cell-directed overexpression of heme oxygenase-1 elevates blood pressure through attenuation of nitric oxide-induced vasodilation in mice, Epub 2001/07/07, Circ. Res. 89 (1) (2001) 55–62, https://doi.org/10.1161/hh1301.092679. PubMed PMID: 11440978.
[52] C.J. Mingone, M. Ahmad, S.A. Gupte, J.L. Chow, M.S. Wolin, Heme oxygenase-1 induction depletes heme and attenuates pulmonary artery relaxation and guanylate cyclase activation by nitric oxide, Epub 2008/01/08, Am. J. Physiol. Heart Circ. Physiol. 294 (3) (2008) H1244–H1250, https://doi.org/10.1152/ajpheart.00846.2007. PubMed PMID: 18178725; PMCID: PMC2441442.
[53] O. Kitada, T. Kodama, K. Kuribayashi, D. Ihaku, M. Fujita, T. Matsuyama, M. Sugita, Heme oxygenase-1 (HO-1) protein induction in a mouse model of asthma, Epub 2001/10/10, Clin. Exp. Allergy 31 (9) (2001) 1470–1477, https://doi.org/10.1046/j.1365-2222.2001.01179.x. PubMed PMID: 11591199.
[54] A.J. Ammit, A.L. Lazaar, C. Irani, G.M. O'Neill, N.D. Gordon, Y. Amrani, R.B. Penn, R.A. Panettieri Jr., Tumor necrosis factor-alpha-induced secretion of RANTES and interleukin-6 from human airway smooth muscle cells: modulation by glucocorticoids and beta-agonists, Epub 2002/03/29, Am. J. Respir. Cell Mol. Biol. 26 (4) (2002) 465–474, https://doi.org/10.1165/ajrcmb.26.4.4681. PubMed PMID: 11919083.
[55] E.A. Goncharova, P.N. Lim, A. Chisolm, H.W. Fogle 3rd, J.H. Taylor, D. A. Goncharov, A. Eszterhas, R.A. Panettieri Jr., V.P. Krymskaya, Interferons modulate mitogen-induced protein synthesis in airway smooth muscle, Epub 2010/04/13, Am. J. Physiol. Lung Cell Mol. Physiol. 299 (1) (2010) L25–L35, https://doi.org/10.1152/ajplung.00228.2009. PubMed PMID: 20382746; PMCID: PMC2904093.
[56] P. Sandner, D.P. Zimmer, G.T. Milne, M. Follmann, A. Hobbs, J.P. Stasch, Soluble guanylate cyclase stimulators and activators, Epub 2019/01/29, Handb. Exp. Pharmacol. (2019), https://doi.org/10.1007/164_2018_197. PubMed PMID: 30689085.